

Supplementary Information for

Dirac node lines in two-dimensional Lieb lattices

Bo Yang, Xiaoming Zhang and Mingwen Zhao*

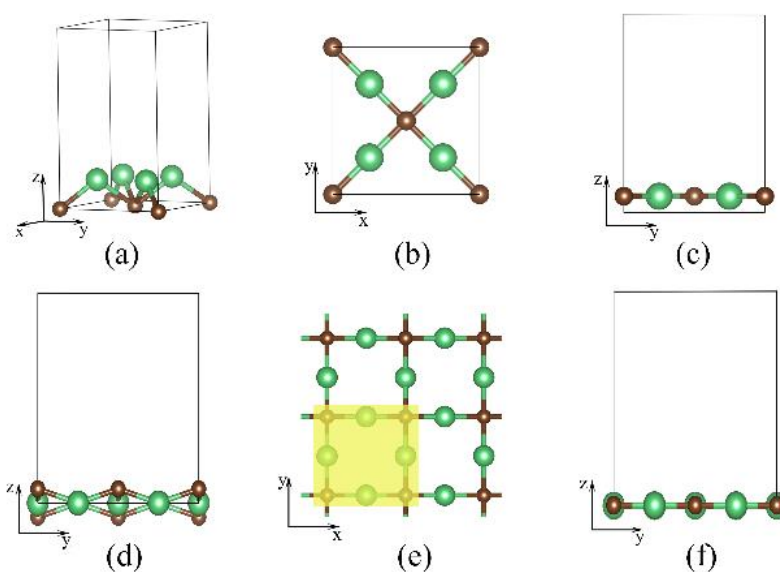


Fig. S1 (a) The (001) bilayer cleaved layer from Be_2C bulk crystal. (b) Top and (c) side views of the optimized structure of Be_2C monolayer. (d) Initial buckled configuration of Be_2C monolayer with the buckling high of 0.5 \AA . (e) Top and (f) side views of optimized Be_2C monolayer starting from the buckled configuration. The results indicate the Be_2C monolayer tends to be the planar configuration.

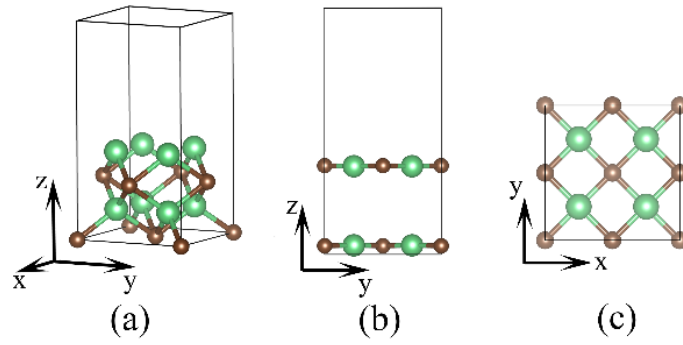


Fig. S2 The (001) four layers cleaved layer from Be₂C bulk crystal. (b) Top and (c) side views of the optimized structure of Be₂C bilayer. The structure relationship between monolayer and bulk crystal indicates the possibility of growing Be₂C monolayer on substrates using bottom-up techniques.

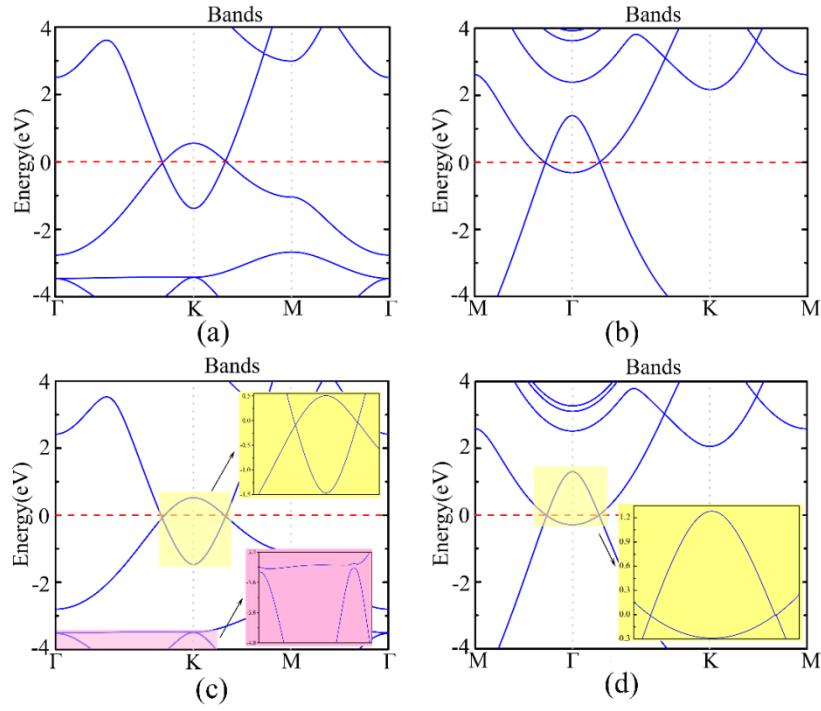


Fig. S3 The electronic band structures of (a) Be_2C and (b) BeH_2 monolayers obtained from first-principles calculations involving SO coupling. The electronic band structures of (c) Be_2C and (d) BeH_2 monolayers with the strength of SO coupling interaction being artificially improved up to ten times order of the magnitude of original one. The energy at the Fermi level was set to zero. These results indicate that both of the DNL states of Be_2C and BeH_2 cannot be gapped and thus are robustness against SO coupling.

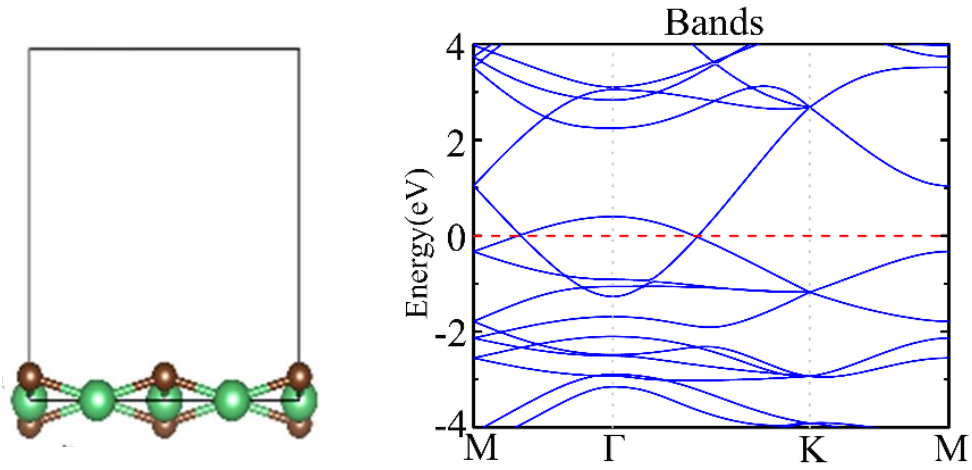


Fig. S4 The electronic band structures of the buckled B₂C monolayer obtained from the first-principles calculations involving SO coupling. The energy at the Fermi level was set to zero. The result indicates the DNL states are robust against the out-of-plane buckling perturbation induced by the substrate effect.

Spin-orbit coupling effects

In order to verify the robustness of DNL against SO interaction, we introduced an intrinsic SO coupling term into the Hamiltonian of the p_z - p_{xy} model. Each site of the Lieb lattice has only one atomic orbital. In this case, there is no on-site spin-orbit coupling term, and the mixing between p_{xy} and p_z is prohibited. Therefore, we only considered the nest-nearest-neighbor (NNN) spin-orbit coupling term.

$$H_{SO} = i\lambda \sum_{\langle\langle i,j \rangle\rangle} \alpha_{i,j} (\vec{d}_{ij}^1 \times \vec{d}_{ij}^2) \cdot \vec{\sigma}_{\alpha\beta} c_{i\alpha}^\dagger c_{j\beta},$$

where λ represents the amplitude for the nest-nearest-neighbor (NNN) spin-orbit-induced interaction. \vec{d}_{ij}^1 and \vec{d}_{ij}^2 are the two unit vectors along the nearest-neighbor Be-Be bonds connecting site i to its next-nearest neighbor j and the term $v_{ij} = (\vec{d}_{ij}^1 \times \vec{d}_{ij}^2) = \pm 1$. $\vec{\sigma}$ is the vector of Pauli matrices.

In momentum space, the spin-orbit term of Hamiltonian is written as follows.

For the p_z + $p_{x,y}$ model:

$$H_k^{SO} = \begin{pmatrix} -2t(\cos(k_x a) + \cos(k_y a)) & 0 & 0 \\ \Delta - i\lambda & -4t' \left(\sin\left(\frac{k_x a}{2}\right) \times \sin\left(\frac{k_y a}{2}\right) \right) & \Delta + i\lambda \end{pmatrix}$$

The energy bands become:

$$E^0 = -2t(\cos(k_x a) + \cos(k_y a))$$

$$E^{(\pm)} = \Delta \pm \left(\lambda^2 + 16t'^2 \sin^2\left(\frac{k_x a}{2}\right) \times \sin^2\left(\frac{k_y a}{2}\right) \right)^{1/2}$$

For the p_z + s model:

$$H_k = \begin{pmatrix} -2t(\cos(k_x a) + \cos(k_y a)) & 0 & 0 \\ \Delta - i\lambda & -4t' \left(\cos\left(\frac{k_x a}{2}\right) \times \cos\left(\frac{k_y a}{2}\right) \right) & \Delta + i\lambda \end{pmatrix}.$$

The energy bands are:

$$E^0 = -2t(\cos(k_x a) + \cos(k_y a))$$

$$E^{(\pm)} = \Delta \pm \left(\lambda^2 + 16t'^2 \cos^2\left(\frac{k_x a}{2}\right) \times \cos^2\left(\frac{k_y a}{2}\right) \right)^{1/2}$$

The DNL arising from the crossing of the two bands cannot be gapped. We also calculated the Z_2 topological invariant based on this Hamiltonian using Fu's strategy and found that it equals to the value without considering SO coupling. This result is reasonable since the band inversion is not related to SO coupling unlike the cases of most TIs